



Comparing the efficiency of WOE and EFB models for spatial pattern analysis of land degradation (case study: Qazvin plain)

Azam Abolhasani¹, Gholamreza Zehtabian¹, Hassan Khosravi¹✉, Omid Rahmati², Esmail Heydari Alamdarloo¹, Paolo D'Odorico³

1- Department of Reclamation of Arid and Mountainous Regions, Faculty of Natural Resource, University of Tehran, Iran. Email: hakhosravi@ut.ac.ir

2- Kurdistan Agricultural and Natural Resources Research and Education Center, Kurdistan, Sanandaj, Iran

3- The University of California, Berkeley, USA

Article Info

Article type:
Research Article

Article history:

Received 16 January 2022

Received in revised form 8

April 2022

Accepted 27 August 2022

Published online 25

September 2022

Keywords:

Capabilit,
Desertification,
GIS,
Predictive accuracy

ABSTRACT

Land degradation is a global natural hazard that can be controlled by distinguishing susceptible areas. Although new approaches for determining areas prone to land degradation are necessary, spatial modeling of this hazard remains a challenge. This study aimed to investigate the efficiency of the weight of evidence (WOE) and evidential belief function (EBF) models for spatial modeling of land degradation in a semi-arid region in Iran. The trend of Net Primary Production (NPP) changes related to 2001-2020, obtained from MOD17A3, was taken into account to specify the inventory of land degradation in the study area. 120 random points were chosen as degraded points in areas with decreasing trend in NPP during 20 years. 70% of the dataset was randomly selected as a training set for the modeling step and 30% of them were selected as the testing set for the validation step. Fifteen geo-environmental factors including temperature, precipitation, slope, aspect, altitude, land use, normalized difference vegetation index, normalized difference salinity index, vegetation soil salinity index, normalized difference moisture index, visible and shortwave infrared drought index, electrical conductivity, and sodium adsorption ratio of groundwater, groundwater table, and annual depletion of groundwater resources were selected as influential factors or independent variables for modeling. The modeling process was done in ArcGIS software after calculating the values of EBF and WOE in excel. And finally, the efficiency of the models was analyzed using the area under the ROC curve. The findings illustrated that EBF with AUC = 0.72 had better performance for spatial modeling of land degradation in the Qazvin plain. Also according to the outputs of both models, north, northeast, northwest, west, southwest, and south of the Qazvin plain were susceptible to LD. The results of this research successfully suggested a new land degradation modeling method that can be used in different areas.

Cite this article: A. Abolhasani, Gh.R. Zehtabian, H. Khosravi, O. Rahmati, E. Heydari Alamdarloo & D'Odorico P. (2022). Comparing the efficiency of WOE and EFB models for spatial pattern analysis of land degradation (Case study: Qazvin plain). DESERT, 27 (2), DOI: 10.22059/jdesert.2022.90830



© The Author(s). A. Abolhasani, Gh.R. Zehtabian, H. Khosravi, O. Rahmati, E. Heydari Alamdarloo & D'Odorico P. Publisher: University of Tehran Press. DOI: 10.22059/jdesert.2022.90830

Introduction

Land degradation (LD) is a negative environmental process, accelerated by human activities (Omuto *et al.*, 2014). Some researchers have defined LD as a general decrease in the productive potential of land (Foster, 2006) or a decline in ecosystem function (Bai *et al.*, 2008). Others have described it as the negative change in land resources due to human activities (UNEP, 1992). Despite different definitions of LD, there is an agreement on the characteristics of this phenomenon: it causes the reduction of the capability of the biological and economic productivity of land (Wieland *et al.*, 2019) and threatens the ecosystem services, global food

security, economic development and the welfare of people around the world (Crossland *et al.*, 2018). Due to its impacts on food production, water supply, energy supply, and ecosystem services (Ewunetu *et al.*, 2021), LD has become a critical problem globally. According to the UNCCD¹ (2015), about 25% of Earth's land area is severely degraded or undergoing degradation. Both human activities, e.g., land-use/land-cover change, and natural factors, e.g., climate change, influence LD (Haghighi *et al.*, 2021). According to the literature, many studies have been done to assess, monitor, and detect sensitive areas to LD utilizing different methods. Mapping LD enables managers and decision-makers to ascertain susceptible areas to LD and make important decisions.

Most previous studies, assessing LD, have utilized various models such as IMDPA² and MEDALUS³ (Boudjemline and Semar, 2018; Právělie *et al.* 2017; Rezaipoorbaghedar, 2015; Mesbahzadeh *et al.*, 2013) or GIS and RS techniques (Bedoui *et al.*, 2020; Mariano *et al.* 2018; Cerretelli *et al.* 2018). Recently, few studies have been done for spatial modeling and assessing land degradation using data mining techniques such as machine learning algorithms. Abolhasani *et al.* (2022) modeled land degradation in the Qazvin plain using machine learning algorithms and concluded that random forest was the best model for modeling LD in the Qazvin plain. Haghighi *et al.* (2021) used human-induced, and geoenvironmental variables and machine learning algorithms to map LD risk in the Pole-Doab watershed, Iran, and concluded that machine learning techniques can help policymakers prioritize land and water conservation efforts. Yousefi *et al.* (2021) applied three machine learning models to assess LD in the rangelands of the Alborz Mountains in Firozkuh County, Iran, and showed that machine learning techniques are a proper approach for estimating rangeland status all over the world. Moradi *et al.* (2020) assessed vulnerability, hazard, and risk of land degradation using machine learning models and remote sensing and showed that machine learning techniques have better performance than remote sensing.

So far, to the best of our knowledge, the applicability of statistical models has not been entirely explored in the context of land degradation and there is not enough study in this field while many studies have been done for modeling other natural hazards such as flood, landslide, etc. using these models (Chen *et al.*, 2019; Tehrany *et al.*, 2017). Also, previous studies in the field of LD modeling have utilized field surveys to determine LD sites. Therefore, the present study proposes a new conceptual framework for spatial modeling of land degradation based on the trends of changes in Net Primary Production (NPP) and statistical models including the Weight of Evidence function (WoE) and Evidential Belief Function (EBF). NPP is the Gross Primary Production (GPP) minus the carbon lack of plant breathing, which is the main index to show the function of ecosystems (Pan *et al.*, 2021). The main objectives of the research were (1) spatial modeling of LD in the Qazvin plain which is considered a critical plain, and (2) comparison of the performance of WoE and EBF models for determining LD susceptibility using area under the ROC curve (AUC). The results of the study can help managers and decision-makers to conserve land sustainability.

Material and methods

Study area

Qazvin plain is located between 49° 10' to 50° 40' eastern longitude and 35° 20' to 36° 30' northern latitude (fig 1). The area of the plain is 9500 Km² and its maximum and minimum altitude are respectively about 2971 m and 950 m. The average annual rainfall of this region

¹ United Nations Convention to Combat desertification

² Iranian Model of Desertification Potential Assessment

³ Mediterranean Desertification and Land Use

varies from 210 mm in the eastern parts to more than 550 mm in the northeastern parts. Also, the minimum and maximum of the average annual temperature are respectively about 2 °C and 18 °C. Based on DeMartonne's classification, most of the climatic zone of the plain is cold semi-arid.

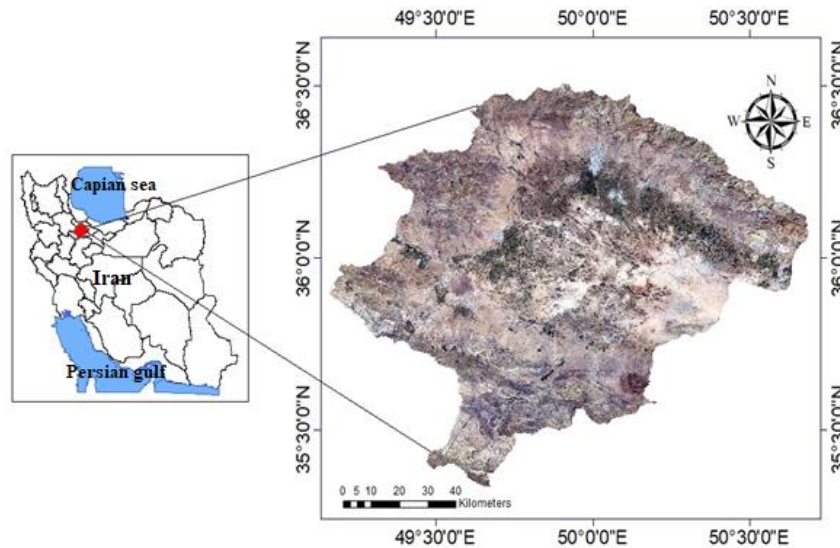


Figure 1. Location of the study area (Qazvin plain, Iran)

Methodology

Inventory factors

To model the LD capability of Qazvin plain, the LD inventory of the study area was ascertained in the first step, utilizing the trend of changes in Net Primary Productivity (NPP). For this aim, the annual NPP related to 2001- 2020 was obtained using MOD17A3. Then, the trend of changes in NPP was determined using the Mann-Kendall trend test in TerrSet software. Locations with constant or increasing trends of NPP were considered non-degraded areas and sites with decreasing trends of NPP were considered degraded locations. 120 random points were chosen in degraded areas. 70% of these sites (84 sites) were randomly chosen as the training set and the remainder (36 sites) of them were selected as the validation set. It should be noted that agricultural lands, urban areas, salt lands, and bare lands were ignored in selecting degradation points and the locations were randomly selected out of these land uses (fig 2).

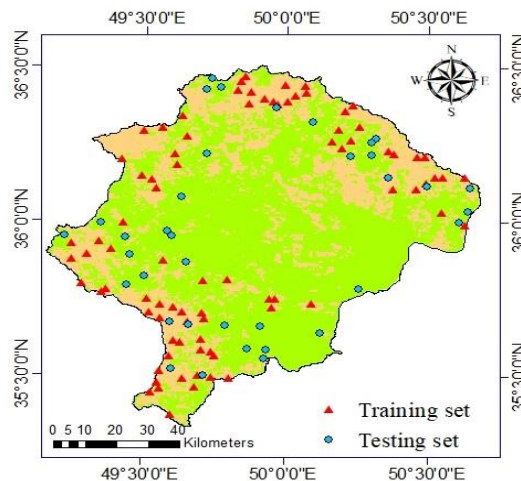


Figure 2. Training and testing set for spatial modeling of land degradation

Influential factors

Due to the complexity of land degradation, there are no universal guidelines for selecting the exact variables that influence this phenomenon. But, according to different studies in this field, the most usual variables which influence LD are soil salinity (Sadeghiravesh *et al.*, 2021), vegetation cover (Kirui *et al.*, 2021), rainfall (Zhang *et al.*, 2020), etc. In this study, according to the studies in the field of land degradation and desertification, slope, altitude, aspect, vegetation index (NDVI⁴), soil salinity indices (NDSI⁵, VSSI⁶), soil moisture indices (NDMI⁷, VSDI⁸), land-use, precipitation, temperature, EC, and SAR of groundwater, groundwater level, and annual groundwater decline were selected as influential factors or independent variables for modeling LD. Information layers of topographic factors were derived from ASTER DEM with a 30*30 m cell size. Meteorological data and groundwater features were obtained from Iran Meteorological Organization and Iran Water Resources Management Organization, respectively. The averages of the precipitation, temperature, EC, SAR, annual groundwater decline and groundwater level related to 2010-2019 were calculated and then interpolated in ArcGIS. Information layers of NDVI, NDSI, VSSI, NDMI, and VSDI indices were also prepared using remote sensing technique (Landsat 8) and ArcGIS software. The land use layer was obtained from the basic map of Forest, Range, and Watershed Management of Iran and then checked as much as possible using google earth and field visits (fig 3).

The name of various land uses is shown in table (1).

Table 1. Various land uses

Number of land use	Name of land use
1	Agricultural lands
2	Dry farming
3	Garden
4	Good rangelands
5	Poor rangelands
6	Urban areas
7	Poor rangelands- Fallow
8	Mid-rangelands
9	Bare lands
10	Dry farming- Mid-rangelands
11	Poor rangelands- Garden
12	Wetlands-salt lands
13	Poor rangelands- Dry farming

According to the determination coefficient, there was no correlation between NDSI and VSSI, and also NDMI and VSDI, therefore, we used these indices in the model simultaneously (fig 4).

⁴. Normalized Difference Vegetation Index

⁵. Normalized Difference Salinity Index

⁶. Vegetation Soil Salinity Index

⁷. Normalized Difference Moisture Index

⁸. Visible and Shortwave infrared Drought Index

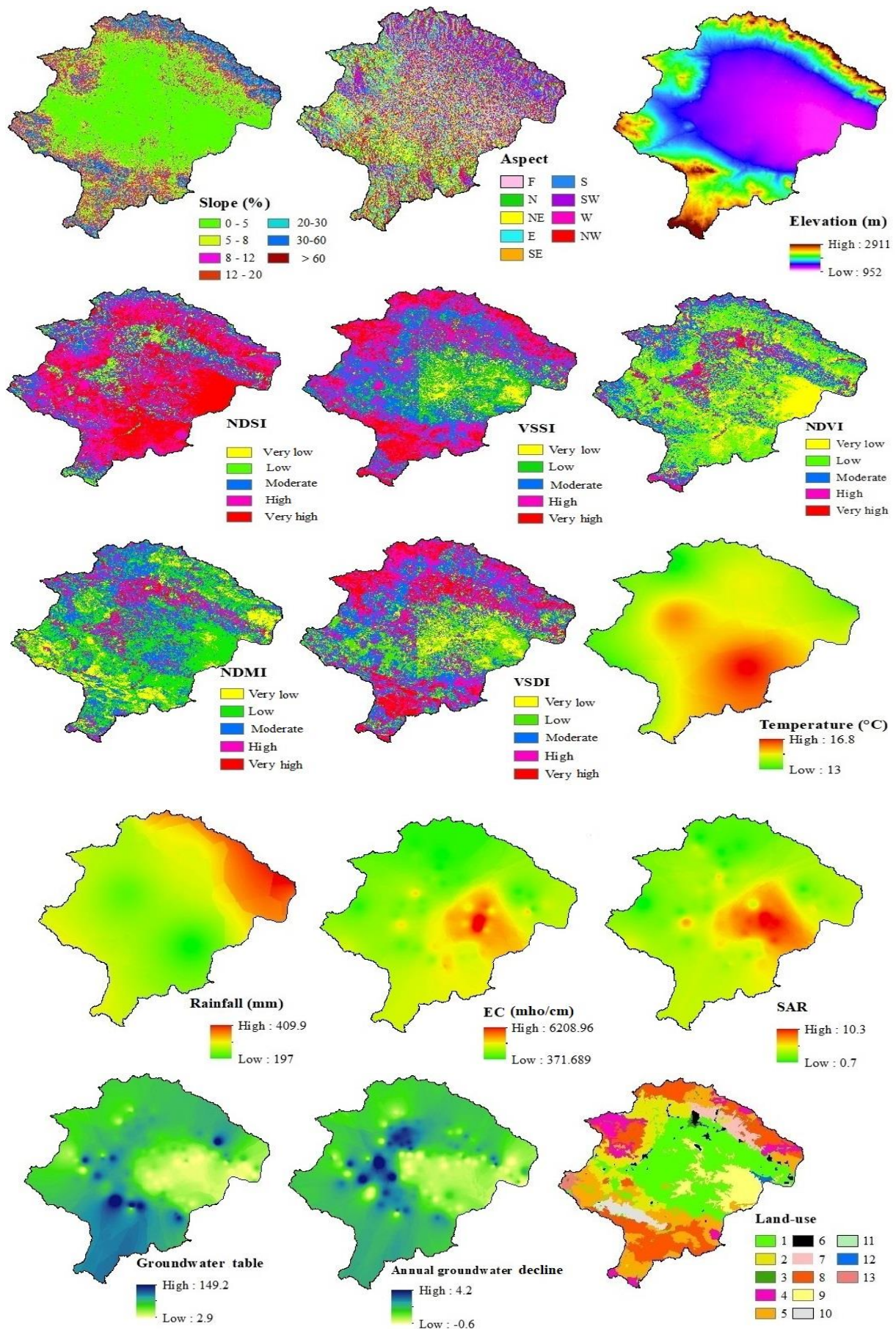


Figure 3. Independent variables influencing LD

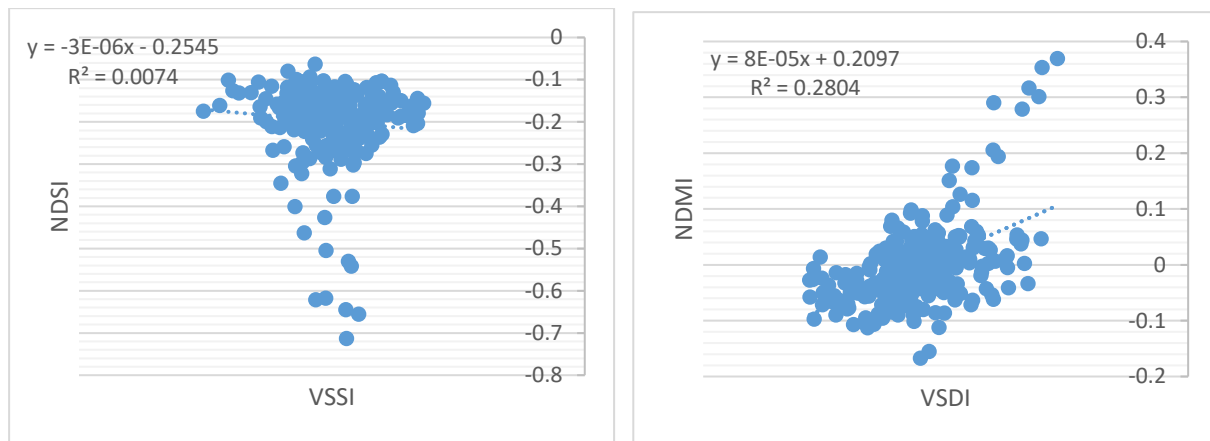


Figure 4. Coefficient of determination between NDSI-VSSI and NDM-VSDI

Modeling

LD capability maps were generated utilizing EBF and WOE methods. EBF, known as the Dempster-Shafer theory developed by Dempster (1976), is a generalization of the Bayesian theory of subjective probability (Tehrany *et al.*, 2017). It has relative flexibility in accepting uncertainty and also the capacity to combine beliefs from multiple sources of evidence (Feizizadeh and Blaschke 2014). Parameters of the EBF model are calculated using equations (1) to (5).

$$\text{Belief (Bel)} = \frac{Bel_1 + Bel_2 + \dots + Bel_n}{B} \quad (1)$$

$$\text{Disbelief (Dis)} = \frac{Dis_1 + Dis_2 + \dots + Dis_n}{B} \quad (2)$$

$$\text{Uncertainty (Unc)} = \frac{\sum_{i=1}^n (Unc_{i-1} Unc_i + Bel_{i-1} Unc_i + Bel_i Unc_{i-1} + Dis_{i-1} Unc_i + Dis_i Unc_{i-1})}{B} \quad (3)$$

$$\text{Plausibility (Pls)} = Bel + Unc \quad (4)$$

$$B = 1 - \sum_{i=2}^n (Bel_{i-1} Dis_i - Dis_{i-1} Bel_i) \quad (5)$$

Where n is the number of factors, Bel is the degree of confidence, Dis is the degree of no confidence, Unc is the degree of uncertainty, pls is the degree of plausibility between 0 and 1. Bel_n is the degree less than confidence for any factor, Dis_n is the degree of no confidence for any factor, and Unc_n is the degree of uncertainty for any factor.

WOE is also a data-driven statistical method based on Bayesian statistics (Thongley and Chaiwiwa, 2020). It depends on the calculation of W^+ and W^- which are positive and negative weights respectively (equations 6,7, and 8).

$$W^+ = \ln \frac{p\{B|A\}}{p\{B|\bar{A}\}} \quad (6)$$

$$W^- = \ln \frac{p\{\bar{B}|A\}}{p\{\bar{B}|\bar{A}\}} \quad (7)$$

Where B is the presence of the influential factor, \bar{B} is the absence of the influential factor, A is the presence of LD and \bar{A} is the absence of LD. To measure the spatial correlation between LD and the influential factors W_f is calculated.

$$W_f = W^+ - W^- \quad (8)$$

Validating

Validation is performed in any modeling procedure to specify whether the results of the utilized model are accurate enough or not (Robinson, 2014). In the current study, the efficiency of the models was evaluated using AUC, the area under the receiver operating characteristic curve (ROC). AUC can distinguish the models' susceptibility (Youssef *et al.*, 2016) and compare the

performance between two or more alternative tests (Yang *et al.*, 2017). In this study, the ROC curve was prepared using MedCalc software. The rule for interpreting the AUC value is illustrated in table (2).

Table 2. AUC values (Yesilnacar, 2005)

AUC values	Test quality
0.5 – 0.6	Poor (Unsatisfactory)
0.6 – 0.7	Average (Satisfactory)
0.7 – 0.8	Good
0.8 – 0.9	Very good
0.9 - 1	Excellent

Results

Land degradation capability maps generated using EBF and WOE models are demonstrated in figure (5). The LD probability ranges from 0 to 1, with 0 representing no probability and 1 representing 100% probability. According to both models, north, northeast, northwest, west, southwest, and south of the Qazvin plain are susceptible to LD.

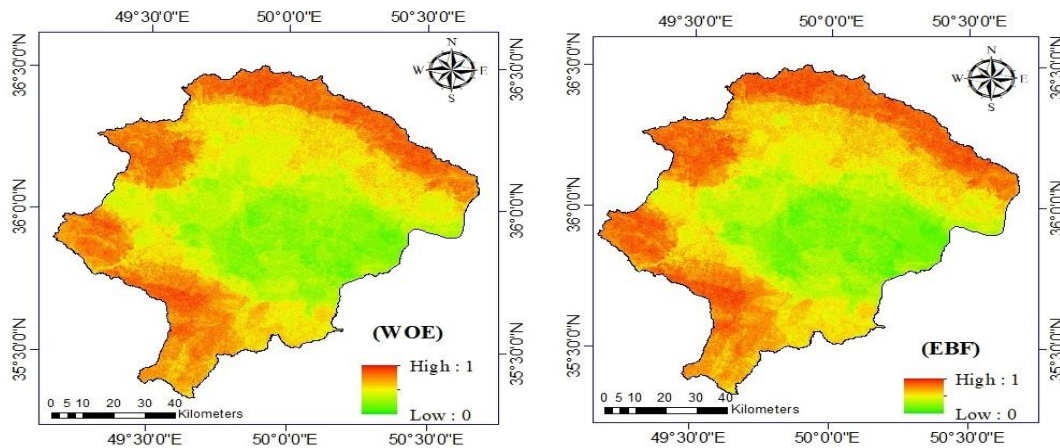


Figure 5. Land degradation capability

The susceptibility maps of LD were also classified into very low, low, moderate, high, and very high classes using the natural break method in ArcGIS (fig 6). According to the findings, high and very high classes of LD belonged to the north, northeast, northwest, west, southwest, and south of the study area which mainly include good, moderate, and poor rangeland.

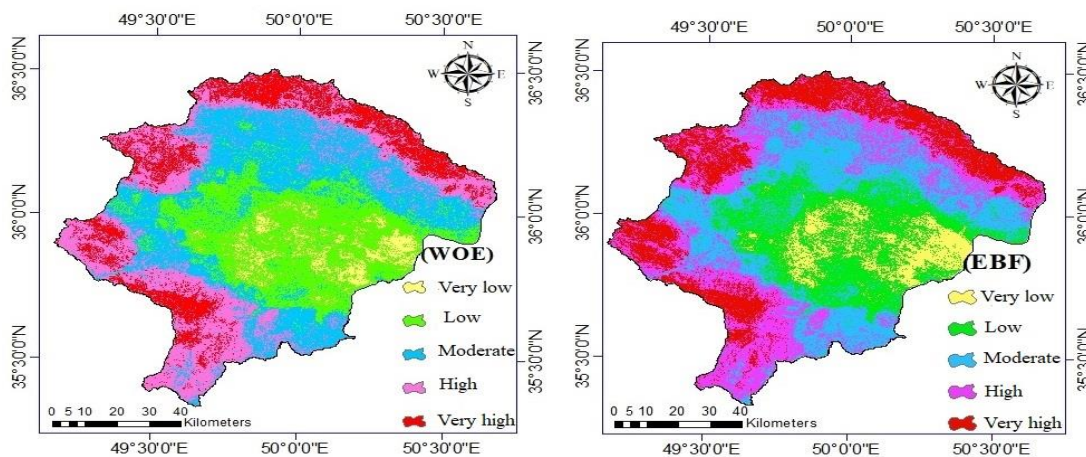


Figure 6. Classification of land degradation capability

The estimated WOE and EBF for 15 land degradation influential factors are shown in tables (3) and (4). The WOE and EBF results on soil salinity indices showed that the range of NDSI between 0.6 and 0.8 and the range of VSSI between 0.8 and 1 received the most value. The outputs on vegetation cover using both WOE and EBF models indicated that classes of 0.4-0.6 gained the most weight. Regarding the soil moisture indices, the classes of 0-0.2 of NDMI and the classes of 0.8-1 of VSDI received the highest EBF value while classes of 0.4-0.6 of NDMI and VSDI acquired the most value using the WOE model. The highest WOE and EBF values were related to the west class of the aspect layer. For the slope layer, the most EBF value was related to the class of more than 60% and the highest WOE value was related to the class of 30-60%. The results on altitude showed that the most EBF weight belonged to the class of more than 2000 m and the highest WOE weight was related to the classes of 1500-2000 and 2000-2500 m. For rainfall factor, the classes of 300-350 mm received the highest EBF and WOE values. The findings on temperature revealed that the most values of EBF and WOE were respectively related to the classes of less than 14 °C and 14-15 °C. For qualitative features of groundwater, the most EBF value was related to the class of less than 2 of SAR and the class of less than 2000 mho/cm of EC. Also, the highest WOE weights belonged to the classes of 2-4 of SAR and the class of less than 2000 mho/cm of EC. The classes of 0.6-1.6 m of annual groundwater drop received the highest EBF and WOE values. In terms of the groundwater table, the class of more than 120 m and the classes of 40-60 m had the highest EBF and WOE values, respectively. Also for the land use layer, the highest value of EBF and WEO was related to the sum of good, moderate, and poor rangelands.

Table 3. Correlation between land degradation and influential factors using the EBF model

Factors	Class	No. of pixels in domain	No. of degradation	Bel (belief)
NDSI	0-0.2	317053	2	0.1780
	0.2-0.4	830777	3	0.1019
	0.4-0.6	2146607	20	0.2630
	0.6-0.8	3623959	35	0.2726
	0.8-1	3671189	24	0.1845
VSSI	0-0.2	775482	1	0.0355
	0.2-0.4	1862225	1	0.0148
	0.4-0.6	3179429	23	0.1991
	0.6-0.8	3172451	31	0.2690
	0.8-1	1599998	28	0.4817
NDVI	0-0.2	2223972	12	0.1582
	0.2-0.4	4388896	40	0.2671
	0.4-0.6	2565283	28	0.3199
	0.6-0.8	1022560	1	0.0287
	0.8-1	388874	3	0.2261
NDMI	0-0.2	1441654	17	0.3221
	0.2-0.4	4436524	30	0.1847
	0.4-0.6	2983954	31	0.2838
	0.6-0.8	1288641	4	0.0848
	0.8-1	438812	2	0.1245
VSSI	0-0.2	775482	1	0.0355
	0.2-0.4	1862225	1	0.0148
	0.4-0.6	3179429	23	0.1991
	0.6-0.8	3172451	31	0.2690
	0.8-1	1599998	28	0.4817
Aspect	Flat	664101	1	0.0213
	North	981277	11	0.1584
	Northeast	1435746	10	0.0984
	East	1393955	6	0.0608
	Southeast	1325186	14	0.1492
	South	1484309	11	0.1047

	Southwest	1294949	8	0.0873
	West	1043596	15	0.2030
	Northwest	966466	8	0.1169
Slope	0-5	5526478	18	0.0282
	5-8%	1486908	12	0.0699
	8-12%	1119021	13	0.1006
	12-15%	1143071	13	0.0985
	15-30%	703701	11	0.1354
	30-60%	558625	15	0.2326
	>60%	51781	2	0.3346
Altitude	<1000	16	0	0.0000
	1000-1500	6354211	17	0.0446
	1500-2000	3156856	45	0.2378
	2000-2500	1034488	21	0.3386
	>2500	44014	1	0.3790
Rainfall	<250	2996929	6	0.0540
	250-300	5355084	49	0.2466
	300-350	1096310	15	0.3688
	>350	1141262	14	0.3306
Temperature	<14	1203692	14	0.3928
	14-15	5140175	54	0.3548
	15-16	3155296	12	0.1284
	>16	1090422	4	0.1239
SAR	<2	1129229	14	0.4802
	(2-4)	5900759	64	0.4201
	(4-6)	2333135	6	0.0996
	(6-8)	936530	0	0.0000
	>8	289932	0	0.0000
EC	<2000	6862771	65	0.6449
	2000-4000	3642573	19	0.3551
	>4000	84241	0	0.0000
Groundwater table	<20	866033	0	0.0000
	20-40	1735681	4	0.0331
	40-60	3899705	40	0.1473
	60-80	2754863	25	0.1303
	80-100	1228441	14	0.1636
	100-120	77556	0	0.0000
	>120	27306	1	0.5258
Annual groundwater decline	<0.6	1474865	1	0.0471
	0.6-1.6	7620330	78	0.7105
	1.6-2.6	1431472	5	0.2424
	2.6-3.6	54830	0	0.0000
	>3.6	8088	0	0.0000
Land use	Agriculture	3156493	0	0.0000
	Garden	69000	2	0.2569
	Bareland	893447	0	0.0000
	Dry farming	1251288	6	0.0425
	Good rangeland	640268	7	0.0969
	Dry farming- mid rangeland	277143	3	0.0960
	Dry farming- poor rangeland	112354	2	0.1578
	Follow- poor rangeland	363605	2	0.0488
	Wetland-salt land	37431	0	0.0000
	Mid rangeland	1909261	35	0.1625
	Poor rangeland	1726758	27	0.1386
	Urban area	152537	0	0.0000

Table 4. Correlation between land degradation and influential factors using the WOE model

Factors	Class	No. of pixels in domain	No. of degradation	W_f
NDSI	0-0.2	317053	2	-0.34
	0.2-0.4	830777	3	-1.44
	0.4-0.6	2146607	20	0.48
	0.6-0.8	3623959	35	0.61
	0.8-1	3671189	24	-1.73
VSSI	0-0.2	775482	1	-1.88
	0.2-0.4	1862225	1	-2.87
	0.4-0.6	3179429	23	-1.02
	0.6-0.8	3172451	31	0.73
	0.8-1	1599998	28	4.14
NDVI	0-0.2	2223972	12	-1.69
	0.2-0.4	4388896	40	1.15
	0.4-0.6	2565283	28	1.93
	0.6-0.8	1022560	1	-2.17
	0.8-1	388874	3	-0.05
NDMI	0-0.2	1441654	17	1.75
	0.2-0.4	4436524	30	-1.14
	0.4-0.6	2983954	31	1.77
	0.6-0.8	1288641	4	-1.99
	0.8-1	438812	2	-0.80
VSDI	0-0.2	899690	1	-2.03
	0.2-0.4	2330924	7	-2.87
	0.4-0.6	3086367	34	2.26
	0.6-0.8	2766443	24	0.51
	0.8-1	1506161	18	1.87
Aspect	Flat	664101	1	-1.70
	North	981277	11	1.20
	Northeast	1435746	10	-0.44
	East	1393955	6	-1.60
	Southeast	1325186	14	1.14
	South	1484309	11	-0.24
	Southwest	1294949	8	-0.75
	West	1043596	15	2.41
Northwest	966466	8	0.13	
Slope	0-5	5526478	18	-5.22
	5-8%	1486908	12	0.06
	8-12%	1119021	13	1.45
	12-15%	1143071	13	1.37
	15-30%	703701	11	2.32
	30-60%	558625	15	4.78
	>60%	51781	2	2.24
Altitude	<1000	16	0	0
	1000-1500	6354211	17	-6.54
	1500-2000	3156856	45	4.57
	2000-2500	1034488	21	4.46
	>2500	44014	1	1.05
Rainfall	<250	2996929	6	-3.86
	250-300	5355084	49	1.42
	300-350	1096310	15	2.22
	>350	1141262	14	1.72
Temperature	<14	1203692	14	1.52
	14-15	5140175	54	2.84
	15-16	3155296	12	-3.00
	>16	1090422	4	-1.62
SAR	<2	1129229	14	1.76
	(2-4)	5900759	64	3.64
	(4-6)	2333135	6	-3.07

	(6-8)	936530	0	0.00	
	>8	289932	0	0.00	
EC	<2000	6862771	65	2.37	
	2000-4000	3642573	19	-2.24	
	>4000	84241	0	0.00	
Groundwater table	<20	866033	0	0.00	
	20-40	1735681	4	-2.67	
	40-60	3899705	40	2.03	
	60-80	2754863	25	0.78	
	80-100	1228441	14	1.44	
	100-120	77556	0	0.00	
	>120	27306	1	1.53	
Annual groundwater decline	<0.6	1474865	1	-2.58	
	0.6-1.6	7620330	78	3.83	
	1.6-2.6	1431472	5	-1.96	
	2.6-3.6	54830	0	0.00	
	>3.6	8088	0	0.00	
Land use	Agriculture	3156493	0	0.00	
	Garden	69000	2	1.84	
	Bare land	893447	0	0.00	
	Dry farming	1251288	6	-1.31	
	Good rangeland	640268	7	0.88	
	Dry farming- mid rangeland	277143	3	0.55	
	Dry farming- poor rangeland	363605	2	-0.53	
	Follow- poor rangeland	37431	0	0.00	
	Wetland-salt land	1909261	35	5.32	
	Mid rangeland	1726758	27	3.80	
	Poor rangeland				
	Urban area				

Evaluating the efficiency of the models demonstrated that the AUC values of EBF and WOE models were respectively 0.72 and 0.69 (fig 7). According to the results, the EBF model had a better performance than the WOE model in spatial modeling of land degradation in the Qazvin plain.

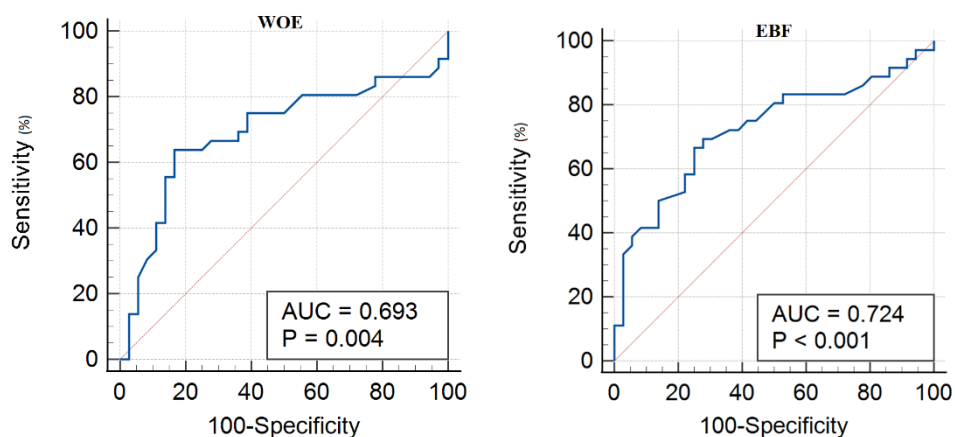


Figure 7. AUC of the models using the training dataset

Discussion

Although new different approaches such as machine learning algorithms have been used for assessing LD capability, the application of WOE and EBF models has not been tested in this field. In this research, a comparative estimation of EBF and WOE statistical models was undertaken to map LD capability in the Qazvin plain and the results of the models were validated using AUC. Based on AUC values, the EBF model had a better proficiency than the WOE model for modeling LD capability in the study area.

The EBF results on soil salinity illustrated that the class of moderate to high soil salinity had a strong correlation with LD in the Qazvin plain. These findings prove that soil salinity has a specific effect on LD in our study area and are consistent with Moradi *et al.* (2020) and Hailu and Mehari (2021) who stated that soil salinity is one of the most significant factors in LD. Regarding topographic factors, slope and altitude had a direct correlation with LD in the Qazvin plain, and susceptible areas to LD are mostly highlands with 15% slope and above. The altitude factor not only has a role in soil evolution directly but also affects important atmospheric parameters and is considered a climate change factor at the regional level and a key factor in land degradation (Jokar Sarsangi *et al.*, 2008). Soil and land degradation are also directly related to the land slope and with an increase in slope, the intensity of erosion and degradation also increases (Ziadat and Timeh, 2013). The outputs of WOE and EBF also showed that the sum of good, moderate, and poor rangelands received the most value among various classes of land use and had a significant role in LD in the Qazvin plain. In addition, the vulnerable areas with the highest LD susceptibility are mostly rangelands especially those with good and medium quality. These land uses, located at high altitudes and steep slopes are susceptible to land degradation maybe because of livestock grazing. Soil trampling and reduction of vegetation cover due to grazing, have exposed these areas to land degradation. These findings are in line with the results of Donovan and Monaghan (2021), Narantsetseg *et al.* (2018), and Goudie (1990) who stated that grazing pressures increase soil erodibility and impact vegetation composition and reduction. The class of land degradation susceptibility was low for bare lands, located in the central parts of the plain because bare lands are now degraded and have no plants or a very poor density of plants.

Conclusion

This research was done to map LD capability using EBF and WOE statistical models in Qazvin plain which has a critical condition. The main conclusion of this study are as follows:

- Based on AUC values, the EBF model's performance for modeling LD in Qazvin plain was better than the WOE's.
- According to the maps of LD capability, the north, northeast, northwest, west, southwest, and south of the Qazvin plain were susceptible to LD that mainly consisted of rangelands of good, moderate, and poor quality.

It is necessary to mention that the derived correlation between the influential factors and LD using EBF and WOE is specific to this research and applying these models in other regions may lead to different results.

References

- Abolhasani A, Zehtabian G, Khosravi H, Rahmati O, Heydari Alamdarloo E, D'Odorico P. 2022. A new conceptual framework for spatial predictive modeling of land degradation in a semi-arid area. *Land Degradation & Development*, 33(17); 3358-3374.
- Bai ZG, Dent DL, Olsson L, Schaepman ME. 2008. Proxy global assessment of land degradation. *Soil use and management*, 24(3); 223-234.

- Bedoui C. 2020. Study of desertification sensitivity in Talh region (Central Tunisia) using remote sensing, GIS, and the MEDALUS approach. *Geoenvironmental Disasters*, 7(1); 1-16.
- Boudjemline F, Semar A. 2018. Assessment and mapping of desertification sensitivity with MEDALUS model and GIS–Case study: basin of Hodna, Algeria. *Journal of water and land development*, 36; (17-26).
- Cerretelli S, Poggio L, Gimona A, Yakob G, Boke S, Habte M, Coull M, Peressotti A, Black H. 2018. Spatial assessment of land degradation through key ecosystem services: the role of globally available data. *Science of the Total Environment*, 628; 539-555.
- Chen W, Sun Z, Han J. 2019. Landslide susceptibility modeling using integrated ensemble weights of evidence with logistic regression and random forest models. *Applied sciences*, 9(1); 171-184
- Crossland M, Winowiecki LA, Pagella T, Hadgu K, Sinclair F. 2018. Implications of variation in local perception of degradation and restoration processes for implementing land degradation neutrality. *Environmental development*, 28: 42-54.
- Donovan M, Monaghan R. 2021. Impacts of grazing on ground cover, soil physical properties and soil loss via surface erosion: A novel geospatial modeling approach. *Journal of Environmental Management*, 287; 112206.
- Ewunetu A, Simane B, Teferi E, Zaitchik B.F. 2021. Mapping and quantifying comprehensive land degradation status using spatial multicriteria evaluation technique in the headwaters area of upper Blue Nile River. *Sustainability*, 13(4); 2244.
- Feizizadeh B, Blaschke T. 2014. An uncertainty and sensitivity analysis approach for GIS-based multicriteria landslide susceptibility mapping. *International Journal of Geographical Information Science*, 28(3); 610-638.
- Foster RH. 2006. Methods for assessing land degradation in Botswana. *Earth and Environment*, 1; 238-276.
- Goudie AS. 1990. *Techniques for desert reclamation*, Chichester: John Wiley & Sons press, 286pp.
- Haghighi AT, Darabi H, Karimidastenaei Z, Davudirad AA, Rouzbeh S, Rahmati O, Sajedi-Hosseini F, Klöve B. 2021. Land degradation risk mapping using topographic, human-induced, and geo-environmental variables and machine learning algorithms, for the Pole-Doab watershed, Iran. *Environmental Earth Sciences*, 80(1); 1-21.
- Hailu B, Mehari H. 2021. Impacts of Soil Salinity/Sodicity on Soil-Water Relations and Plant Growth in Dry Land Areas: A Review. *Journal of Natural Research Science*, 12(3); 1-12.
- Jokar Sarsangi E, Gholami V, Gonbad M.B. 2008. Investigation of the effect of topographic factors on the intensity of soil erosion (Case study: Zaram-Rud watershed), *Journal of Geographical Researches*, 4 (64); 169-177. (In Persian)
- Kirui O.K, Mirzabaev A, von Braun J. 2021. Assessment of Land Degradation on the Ground and from above. *SN Applied Sciences*, 3(3); 1-13.
- Mariano DA, dos Santos CA, Wardlow BD, Anderson MC, Schiltmeyer AV, Tadesse T, Svoboda MD. 2018. Use of remote sensing indicators to assess effects of drought and human-induced land degradation on ecosystem health in Northeastern Brazil. *Remote Sensing of Environment*, 213; 129-143.
- Mesbahzadeh T, Ahmadi H, Zehtabian GR, Sarmadian F. 2013. Assessment and mapping of land degradation in Abuzaydabad, Iran using an IMDPA model with emphasis on land criteria. *Desert*, 18(1); 1-7.
- Moradi E, Khosravi H, Zehtabian GhR, Khalighi Sigaroodi Sh, Cerda A. 2020. The assessment of vulnerability, hazard, and risk of land degradation using data mining techniques in Bakhtegan basin, Ph.D. thesis in combating desertification, faculty of natural resources, University of Tehran. 132pp. (In Persian)
- Narantsetseg A, Kang S, Ko D. 2018. Livestock grazing and trampling effects on plant functional composition at three wells in the desert steppe of Mongolia. *Journal of Ecology and Environment*, 42(1); 1-8.
- Omuto CT, Balint Z, Alim MS. 2014. A framework for national assessment of land degradation in the drylands: a case study of Somalia. *Land degradation & development*, 25(2); 105-119.

- Pan N, Wang S, Wei F, Shen M, Fu B. 2021. Inconsistent changes in NPP and LAI determined from the parabolic LAI versus NPP relationship. *Ecological Indicators*, 131; 108134.
- Prăvălie R, Săvulescu I, Patriche C, Dumitrașcu M, Bândoc G. 2017. Spatial assessment of land degradation sensitive areas in southwestern Romania using modified MEDALUS method. *Catena*, 153; 114-130.
- Rezaipoorbaghedar A, Bahrami H, Rafee Sharifabad J, Khosravi H. 2015. Desertification Assessment using IMDPA model (Case study: Baghedar region, Yazd). *Journal of Arid Regions Geographics Studies*, 5(19); 42-54. (In Persian)
- Robinson S. 2014. *Simulation: The Practice of Model Development and Use*. 2nd edition. Palgrave Macmillan. 392p.
- Sadeghiravesh M.H, Khosravi H, Abolhasani A, Ghodsi M, Mosavi A. 2021. Fuzzy Logic Model to Assess Desertification Intensity Based on Vulnerability Indices. *Acta Polytechnica Hungarica*, 18(3).
- Tabib Mahmoodi F, Ghasemi Dastgerdi N. 2020. Investigating the potential of soil moisture indices in desertification. *Journal of Natural Environment*, 73 (3); 529-542. (In Persian)
- Tehrany MS, Shabani F, Javier DN, Kumar L. 2017. Soil erosion susceptibility mapping for current and 2100 climate conditions using evidential belief function and frequency ratio. *Geomatics, Natural Hazards and Risk*, 8(2); 1695-1714.
- Thongley T, Vansarochana C. 2020. Weight of Evidence Approach for Landslide Susceptibility Mapping: A Case Study at Ossay Watershed Area in Bhutan. *Disaster advances*, 13(9); 1-14
- UNCCD. *Climate change and land degradation: Bridging knowledge and stakeholders Outcomes*. In Proceedings of the UNCCD 3rd Scientific Conference, Cancun, Mexico, 9–12 March 2015.
- UNEP. 1992. *World Atlas of Desertification*. Edward Arnold: London. Wessels KJ, Prince SD, Malherbe J, Small J, Frost PE, VanZyl D. 2007.
- Wieland R, Lakes T, Yunfeng H, Nendel C. 2019. Identifying drivers of land degradation in Xilingol, China, between 1975 and 2015. *Land Use Policy*, 83; 543-559.
- Yang S, Berdine G. 2017. The receiver operating characteristic (ROC) curve. *The Southwest Respiratory and Critical Care Chronicles*, 5(19); 34-36.
- Yesilnacar EK. 2005. *The application of computational intelligence to landslide susceptibility mapping in Turkey*. University of Melbourne, Department, 200.
- Yousefi S, Pourghasemi H.R, Avand M, Janizadeh S, Tavangar S, Santosh M. 2021. Assessment of land degradation using machine-learning techniques: A case of declining rangelands. *Land Degradation & Development*, 32(3); 1452-1466
- Youssef AM, Pourghasemi HR, Pourtaghi ZS, Al-Katheeri MM. 2016. Landslide susceptibility mapping using random forest, boosted regression tree, classification and regression tree, and general linear models and comparison of their performance at Wadi Tayyah Basin, Asir Region, Saudi Arabia. *Landslides*, 13(5); 839-856
- Zhang C, Wang X, Li J, Hua T. 2020. Identifying the effect of climate change on desertification in northern China via trend analysis of potential evapotranspiration and precipitation. *Ecological Indicators*, 112; 106141.
- Ziadat FM, Taimeh AY. 2013. Effect of rainfall intensity, slope, land use, and antecedent soil moisture on soil erosion in an arid environment. *Land Degradation & Development*, 24(6); 582-590.